PATTERN OBSERVATION DURING BED-FORM DEVELOPMENT

Heide Friedrich [1], Bruce W. Melville [2]

1. Department of Civil & Environmental Engineering, The University of Auckland, Private Bag 92019, Auckland, New Zealand. h.friedrich@auckland.ac.nz.
2. Department of Civil & Environmental Engineering, The University of Auckland, Private Bag 92019, Auckland, New Zealand. b.melville@auckland.ac.nz.

Abstract: Most natural patterns exhibit some form of complex behaviour. Underwater bed forms generally start small and appear initially to be disorganized. They grow in height and spacing and become better organized through interactions and mergers between bed forms. For this study, spatial plan-view bed-form development patterns are studied visually. Photographic images of bed-form growth starting from a flat bed in fine uniform sand are obtained in a laboratory flume environment. Various merging and termination processes are identified. Literature review shows that the observed pattern changes during early bed-form development are similar to processes observed for aeolian dune fields.

INTRODUCTION

Hidden from our eyes, bed forms are the result of a feedback mechanism between the flow of water and a movable sediment bed. Commonly bed-form development is studied with the help of spatial or temporal longitudinal profiles of recorded sand-bed elevations. The various lateral merging/termination processes involved are not accounted for in this 2D projection of a 3D event. A complete 3D pattern analysis is necessary in order to better understand the processes that take place during bed-form development and early bed-form growth.

BACKGROUND

Fluvial bed-form pattern

Raudkivi and Witte (1990) addressed the phenomenon of geometrical change of dune dimensions during dune development for the 2D case. Based on Exner's (1925,1931) theoretical concepts, according to which bed forms migrate at speeds inversely proportional to their heights, Raudkivi and Witte (1990) proposed a so-called unification model for bed-form development starting from a flat sand bed. The unification model shows that initially-uniform distributions of the heights of disturbances slowly change into a broad distribution of heights. The change in bed-form size is attributed to the coalescence process. Later papers by Raudkivi (1997, 2006) also refer to the coalescence process during bed-form development. Coleman and Melville (1994) continued to study the coalescence process and showed how bed-form size during growth can be related to migration velocity of bed forms. This study was undertaken in a 15-cm wide laboratory flume, therefore 3D aspects were not disclosed. In contrary to the above mentioned studies, Ditchfield and Best (1990) stated that no relationship between migration velocity and bed-form size exists.

Based on a 3D study of bed-form development in medium sand, Venditti et al. (2005) argued that widespread coalescence does not take place, neither during growth nor equilibrium studies. Instead a crest realignment takes place, which can be mistaken for bed-form coalescence by projecting the bed-form profile into 2D. Additionally, Venditti et al. (2005) report about defects during observations of 3D dune development. During the 2D to 3D dune transition it was observed that the bed-form field appears capable of absorbing a small number of defects. As the number of defects grows with time, the resulting morphological perturbations produce a transition in bed state to 3D forms. These 3D forms continue to evolve, but are seen to be pattern-stable.

Besides the 3D study by Venditti et al. (2005) no other study is known to the authors where underwater bed-form patterns are studied in 3D.

Aeolian bed-form pattern

Due to available aerial photography of aeolian dunes, more studies have focused on the change of pattern of aeolian dunes. Schwämmle and Herrmann (2003) studied barchan sand dunes mathematically and showed how these dunes can traverse through one another, without major changes to their shape. They distinguish between coalescence (both dunes merge into one), breeding (the creation of three baby dunes) and solitary wave behaviours during the fusion of two dunes. A follow-up study (Duran et al., 2005) suggested that additionally a budding scenario (the small dune, after “crossing” the big one, is unstable and splits into two new dunes) can take place. Similar to the budding scenario, Hersen (2005) describes that rather than a simple coalescence behaviour, an absorption/emission process takes place, when a smaller dune merges into a bigger dune, prompting the emission of several small dunes.

From observations in nature and model simulations, Kocurek and Ewing (2005) derived a dune-pattern ordering for natural systems. The ordering system shows dune–dune interactions. Kocurek and Ewing (2005) distinguish five different patterns: a) merging – the simplest interaction, when bed forms are small, diverse in size and closely spaced; b) lateral coalescing of terminations – which can be seen as lateral merging and results in increased crest length; c) defect migration – a crest termination merges with

the downwind crest and results in emission of a new crest termination further downwind; d) repulsion – similar to merging, but once merged results in the emission of another small dune; e) termination creation – whereby at first two crests merge and later a pair of terminations is created.

Essentially, the above mentioned processes as observed for aeolian dunes can be summarized as merging, termination, defect and emission processes, whereby merging can take place in the downwind direction as well as lateral to the wind.

Furthermore, Kocurek and Ewing (2005) distinguish between simple dune-field patterns (one pattern of dunes exists) and complex dune-field patterns (multiple patterns are spatially superimposed). In contrast to the unidirectional flow in laboratory flumes, aeolian dune fields are exposed to changing wind directions, resulting in a simple pattern to represent a single generation of dune-field construction, and a complex pattern to represent multiple generations of construction. Although this approach is not valid for fluvial bed-forms and will not be further discussed in this paper, the phenomena of superposed bed-forms can be studied in a similar way.

Need and objective

Understanding the pattern change during bed-form development as well as pattern changes in equilibrium conditions is necessary in order to be able to increase our understanding of how the turbulent flow field interacts with the movable sediment bed. Currently time-averaged approaches are often (Schindler and Robert, 2005) used in turbulence statistics of flow over bed forms, as constant migration and coalescence of bed forms does not allow the comparison of individual spatial or temporal data series. Besides a conceptual understanding of 3D bed-form development, more studies are needed to identify different scenarios during the 3D development of underwater bed forms.

EXPERIMENTAL SETUP

Flume and instrumentation

The experiments were conducted in a sediment and water recirculating narrow flume in the Fluid Mechanics Laboratory of The University of Auckland. The narrow flume is 0.44-m wide and 12-m long. A bed of uniform (f)ine sand (D_{50}=0.24-mm) was created inside the flume, with a thickness of about 9-cm. The bed material corresponded to a geometric standard deviation of 1.5. Two floodlights were used to create a horizontal observation plane oriented in the longitudinal direction on the channel axis. A digital camera captured images of sediment motion along the observation plane from above. An ADV probe was used to measure a time series of the three components of the instantaneous flow velocity over the initially flat bed, with a sampling frequency of 25 Hz. The sensor was positioned on the centreline of the flume, so that the sampling volume is at 0.368H, H being the water depth, which according to Yalin (1992) corresponds to the water depth of the average flow velocity. Bulk flow velocities were measured. Therefore no information about the critical shear velocity is available for this experimental data set. As soon as the flow in the flume commenced, the data acquisition was started. The experiments were carried out under uniform flow conditions. A series of ten experiments was conducted. Two flow depths were used, a (s)hallow depth of H=15-cm and a (d)eep flow depth of H=19-cm. Flow conditions corresponded to

Reynolds numbers $Re = U_{avg}H/\nu$, in the range from about 45,000 to 115,000, where U_{avg} denotes the mean flow velocity, and ν denotes the fluid kinematic viscosity. Values of the Froude number were in the range from about 0.24 to 0.45. Table 1 shows the bulk flow hydraulics for the 10 experiments. The letter (v) indicates that the experiments are recorded with a video-like setup.

Table 1. Experimental parameters

Experiment	H [m]	D_{50} [mm]	U_{avg} [m/s]	Q [m^3/s]	Fr [-]	Re_m [-]	Re_H [-]	S_B [%]	Total Images [No]	Total Time [hr:min:sec]
vsf8	0.15	0.24	0.29	0.019	0.239	25,865	43,500	0.001	3067	00:28:24
vsf10a	0.15	0.24	0.35	0.023	0.289	31,216	52,500	0.001	1860	00:08:05
vsf10b	0.15	0.24	0.35	0.023	0.289	31,216	52,500	0.001	1800	01:14:38
vsf10d	0.15	0.24	0.35	0.023	0.289	31,216	52,500	0.001	1500	00:14:07
vsf15	0.15	0.24	0.49	0.032	0.404	43,703	73,500	0.001	995	00:05:31
vdf10	0.19	0.24	0.30	0.025	0.220	30,585	57,000	0.001	3790	01:40:41
vdf13	0.19	0.24	0.40	0.033	0.293	40,780	76,000	0.001	1403	00:39:45
vdf15	0.19	0.24	0.45	0.038	0.330	45,878	85,500	0.001	979	00:05:26
vdf18	0.19	0.24	0.54	0.045	0.396	55,054	102,600	0.001	1922	00:10:40
vdf21	0.19	0.24	0.61	0.051	0.447	62,190	115,900	0.001	993	00:05:31

Note: Kinematic viscosity ν=0.000001-m^2/s; Specific gravity S_s=2.65; Critical shear velocity $u_{*c}(D_{50}$=0.24-mm)=0.0132-m/s, Flume Width B=0.44-m

D_{50} Median grain size, H Flow Depth, S_B Flume Slope, U_{avg} Average Flow Velocity, Fr Froude Number, Re Reynolds Number, m Hydraulic Radius (A/2H+B), A Cross-sectional area of the flow, Q Discharge

$$\mathrm{Re}_m = \frac{mU_{avg}}{\upsilon} \qquad \mathrm{Re}_H = \frac{HU_{avg}}{\upsilon}$$

Camera setup

A black-and-white MegaPlus ES 1.0 high-resolution CCD camera was employed to capture the image sequences. The camera was mounted above the flume and centred at 2-m from the outlet section of the flume. The camera is capable of capturing images at 3-Hz (roughly 3 frames/sec) with a resolution of 1008 (horizontal) x 1018 (vertical) pixels per frame. The camera was installed and focused to capture an area of the bed of 0.44-m x 0.44-m, thus capturing events over the whole width of the flume. For this case, a resolution of roughly 0.44-mm/pixel is obtained. To make even minimal sand perturbations visible (Figure 2), light was directed onto the sand bed from both downstream flume sides, at an angle of around 30°. The two floodlights were positioned downstream of the capturing window and oriented to intersect at the camera focal point, such that the lee side is illuminated and the stoss side is in shadow. This resulted in a good highlight for the sand-bed perturbations, which are often in the millimetre scale. The side lighting also helped to produce a glare-free image.

A Plexiglas plate, 0.01-m thick, 0.44-m wide and 1-m long was suspended at the water surface with a beveled edge that faced upstream. During the first experiments problems were encountered with water bubbles collecting underneath the Plexiglas plate

(vsf10a and vsf10b). For the later experiments, care was taken to minimize water bubble collection.

Using the particular camera and computer hard drive, it was possible to record only about $5^{1/2}$ minutes of experimental time. In order to capture events over a longer time frame, it was necessary to stop and restart the experiments once the images from an experimental run had been downloaded to a hard drive.

Individual grain paths could not be discerned due to the low image capturing frequency of 3-Hz. However bulk grain paths could be observed in the captured images and these allow identification of bulk sweep events.

Since the video camera was focused at the initially flattened sand bed, growing features observed on the bed were distorted minimally. Such distortion can be neglected for the qualitative interpretation process used. The images were analyzed in order to identify patterns during bed-form development. Time-lapsed image sequence of the initiation and development of bed forms have been prepared and are being analyzed.

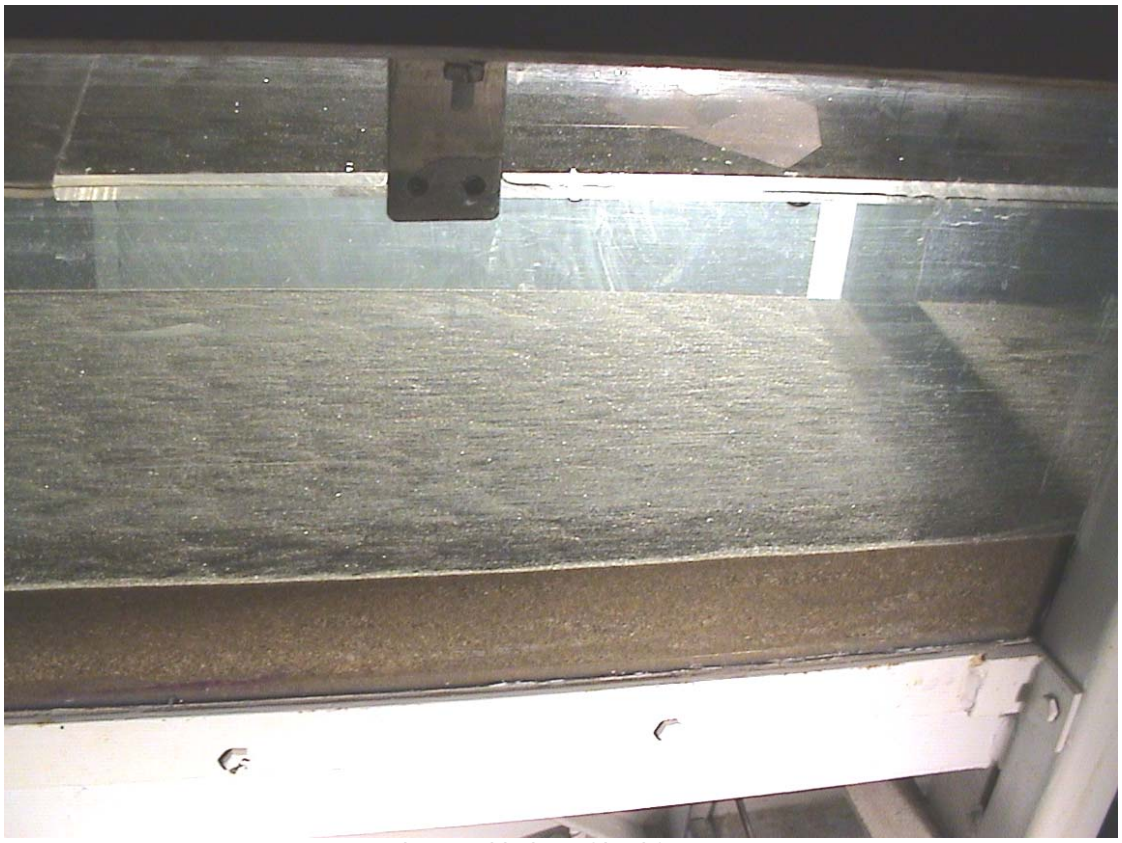

Fig. 2. Initiation of bed forms

RESULTS AND DISCUSSION

In the following Section observed pattern changes during underwater early bed-form growth are qualitatively described. Footage of the camera is used for reference, with each individual photo displaying an area of 0.44-m x 0.44-m of the flume, with water flowing from bottom to top. Each pattern change is discussed in relation to previous known knowledge about fluvial and aeolian bed-form changes.

Merging

Studied as part of the coalescence process in fluvial bed forms, downstream merging is the most well-known pattern changing process. As described in the coalescence process, downstream merging takes place when bed forms are small and closely spaced. Studies of aeolian dunes agree with fluvial bed-form studies, stating that downwind merging takes place when smaller and faster dunes catch up with larger and slower dunes.

Lateral merging (Figure 3) of terminations, neglected in previous 2D fluvial bed-form studies, is a type of merging, which results in increased crest length. It is observed for low flow strengths at the beginning of bed-form generation when individual bed forms are aligned lateral to the flow, prompting one crestline along the flume width. It seems that both downstream and lateral merging result in a decrease in defect density and enable the sand bed to find its stable state for a given flow condition. The observed lateral merging process is similar to the one observed for aeolian dune studies (Kocurek and Ewing, 2005), where it is argued that both downwind as well as lateral merging results in decreasing defect density. It can be seen as a selection process during the growth phase, when bed forms obtain equilibrium shape and sediment transport velocity.

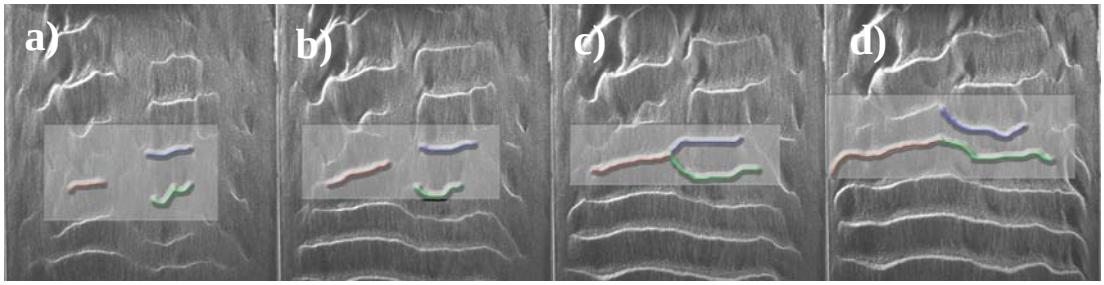

Fig. 3. Merging – experiment vsf8; a) t=0sec, b) t=19sec, c) t=33sec, d) t=56sec.

Termination

In our study, termination of crestlines occurred extensively during the growth period. As Figure 4 shows, a crest is established across the flume width, only to be terminated later, with the original terminated crest upstream (Figure 4a) becoming a full flume-width crest as a result (Figure 4d). Terminations seem to be important in order for the bed-form field do develop. Often a new termination later attaches again with either a downstream or upstream crest, depending on its own sand volume, compared to the neighbouring crests.

Defect migration

Forward defect migration was discussed by Venditti et al. (2005) and is also observed in the present experiments (Figure 5). Once a defect is formed (Figure 5a) it will move

downstream and detach from the original upstream crestline and attach again to the next downstream crestline (Figure 5d). If such a defect creation and migration is seen in 2D, it can be mistaken for a coalescence process, although it is a spatially restricted scenario and does not significantly change the number of bed forms nor the shape of bed forms.

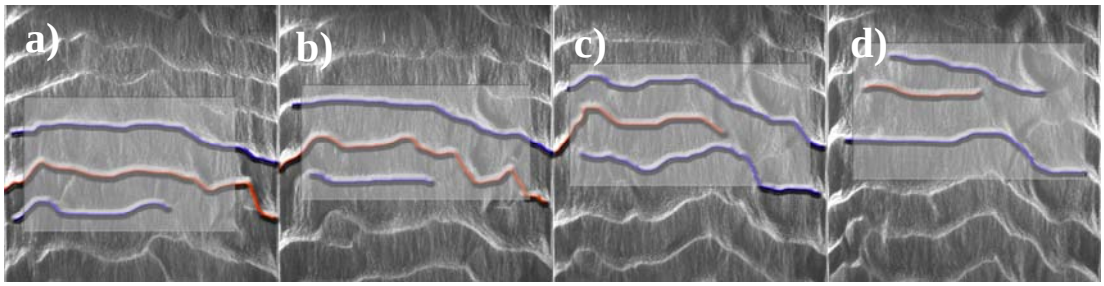

Fig. 4. Termination – experiment vsf15; a) t=0sec, b) t=13sec, c) t=24sec, d) t=39sec.

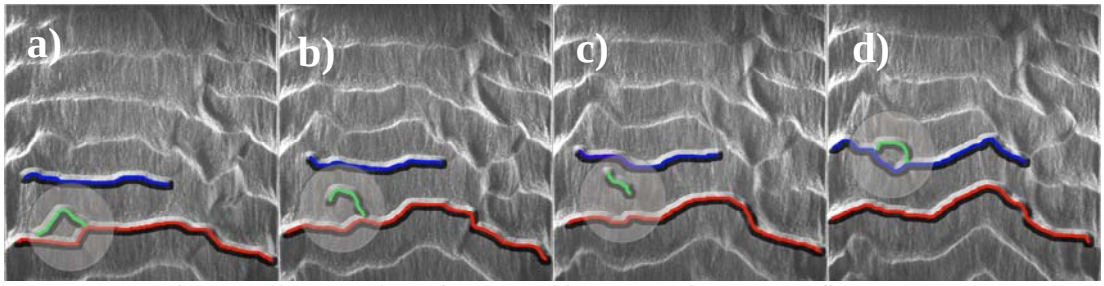

Fig. 5. Defect - vsf15; a) t=0sec, b) t=7sec, c) t=10sec, d) t=15sec.

General observations

During bed-form development several pattern changing processes take place simultaneously (Figure 6 and 7). As Figure 6 shows, lateral merging and termination processes take place concurrently. Figure 6a shows a full flume-width crestline with a y-junction crest upstream of it. During bed-form development, one part of the y-junction terminates (Figure 6b) and attaches to the downstream crest (Figure 6c,d). A brief detachment (termination – Figure 6e,f) follows, before the original y-junction termination attaches with a new termination of the original downstream crest (Figure 6g,h). The new crest stretches again across the flume.

Figure 7 shows an initial lateral merging of the downstream crest (Figure 7a,b), with a simultaneous lateral merging and creation of a new bed feature further upstream (Figure 7b). A short time later (Figure 7c,d,e) the crest downstream of the new bed feature starts to rearrange and consequently terminates, before the new bed feature forms part of the original downstream crest and stretches again across the whole flume width (Figure 7f). Ultimately, the upstream crest terminates, the original new bed feature establishes itself in the merged bed form and the furthest downstream crest starts to merge with the neighbouring upstream crest (Figure7h).

The scenarios discussed above are examples of our observations for early 3D bed-form development. They show the complexities involved during pattern changes. Although no 2D bed-form profiles are available for the visual data set, it is not difficult to see that a lot of the processes are not exposed when analyzing spatial or temporal 2D

bed-form profiles. Pattern descriptions, similar to the ones presented by Kocurek and Ewing (2005), should be adopted for underwater bed-form development studies. The concurrent presence of more than one distinct pattern process (3D merging, termination, defect migration and origin of new crests), as presented in Figures 6 and 7, makes this a challenging task, but if successful should help in our desire to accurately model 3D bed-form development.

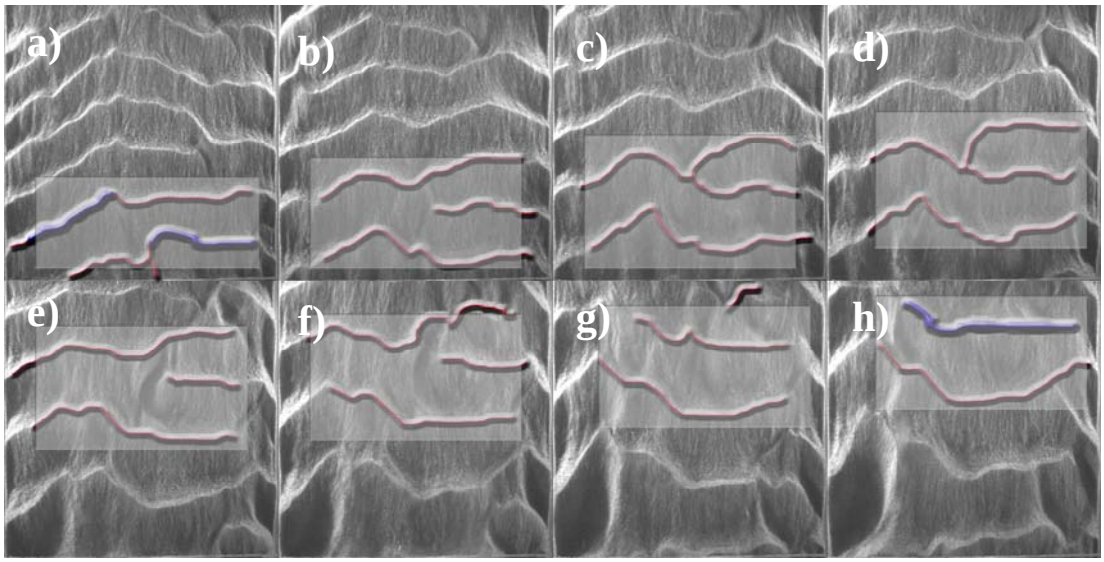

Fig. 6. Termination and merging bed-form interaction – vdf15; a) t=0sec, b) t=22sec, c) t=34sec, d) t=46sec, e) t=57sec, f) t=69sec, g) t=81sec, h) t=92sec.

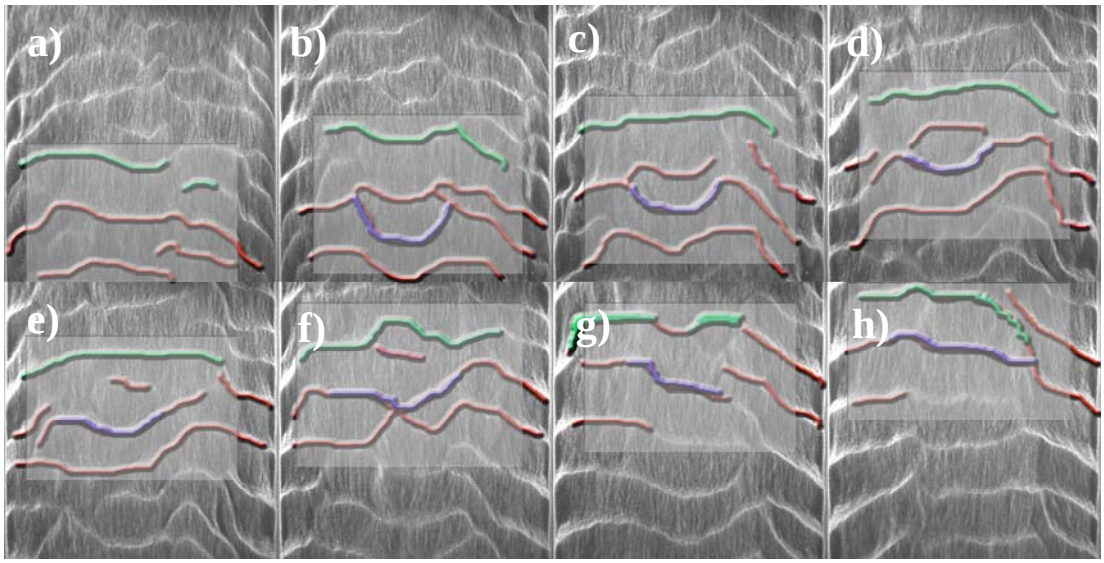

Fig. 7. Bed-form interaction – vdf15; a) t=0sec, b) t=7sec, c) t=13sec, d) t=23sec, e) t=27sec, f) t=34sec, g) t=42sec, h) t=51sec.

CONCLUSION

Recently, Venditti et al. (2005) presented results from bed-form development experiments undertaken in laboratory flumes and focusing on plan-view footage of 3D bed-form growth. Literature research showed that no other plan-view footage of underwater bed-form growth exists. In regards to pattern analysis of bed forms, conceptual models exist, but most are based on 2D analysis of temporal or spatial sand-bed elevation data sets. As Venditti et al. (2005) argued, coalescence theory originating from 2D bed-form growth studies, can also resemble lateral crest realignment when viewed in 2D.

We captured plan-view images of early 3D bed-form growth, starting from a flat sand bed. Processes such as merging, termination and defect migration are qualitatively presented. A literature review of aeolian dune patterns shows that a recent study by Kocurek and Ewing (2005) also identified similar pattern processes. We can conclude that 2D analysis of bed-form growth does not provide sufficient enough information about how bed forms interact with each other.

The research is seen as an important step in improving 3D numerical simulations because it is necessary to know how bed forms react with each other in certain environments. It is generally assumed that based upon a sand volume argument, the formation of a new pattern of small bed forms can proceed more rapidly than reorientation of existing bed forms where the existing bed forms are in equilibrium state for a given flow and the defect density is low. Image sequences from the experiments show that during the complex pattern generation, merging (predominantly), termination and defect migration take place.

This study is restricted by limited flow field information as well as a low frame grabbing frequency of 3-Hz for the camera equipment. Further research is needed to collect a complete visual set of bed-form initiation data for different grain sizes and grain size distributions, and accurate flow field information to correlate the data. Additionally, studies of equilibrium pattern development are required to increase our understanding of how merging processes take place once equilibrium shape and migration velocities are reached.

ACKNOWLEDGEMENTS

The research was partly funded by the Marsden Fund (UOA220) administered by the New Zealand Royal Society. The authors wish to acknowledge the support by the technical staff, Geoff Kirby and Jim Luo.

REFERENCES

Exner, F. M. (1925). "Ueber die Wechselwirkung zwischen Wasser und Geschiebe in Fluessen." *Sitzungsberichte der Akademic der Wissenschaften*, 165-180.

Exner, F. M. (1931). "Zur Dynamik der Bewegungsformen auf der Erdoberflaeche." *Ergebnisse Der Kosmischen Physik.*

Coleman, S. E., and Melville, B. W. (1994). "Bed-Form Development." *Journal of Hydraulic Engineering*, 120(4), 544-560.

Ditchfield, R., and Best, J. (1990). "Development of Bed Features - Discussion." *Journal of Hydraulic Engineering*, 116(9), 647-655.

Duran, O., Schwämmle, V., and Herrmann, H. (2005). "Breeding and solitary wave behaviour of dunes." *Physical Review E - Statistical, Nonlinear, and Soft Matter Physics*, 72(2), 1-5.

Hersen, P. (2005). "Flow effects on the morphology and dynamics of aeolian and subaqueous barchan dunes." *J. Geophys. Res.*, 110, F04S07.

Kocurek, G., and Ewing, R. C. (2005). "Aeolian dune field self-organization - Implications for the formation of simple versus complex dune-field patterns." *Geomorphology*, 72(1-4), 94-105.

Raudkivi, A. J., and Witte, H.-H. (1990). "Development of Bed Features." *Journal of Hydraulic Engineering*, 116(9), 1063-1079.

Raudkivi, A. J. (2006). "Transition from ripples to dunes." *Journal of Hydraulic Engineering*, 132(12), 1316-1320.

Schindler, R. J., and Robert, A. (2005). "Flow and turbulence structure across the ripple-dune transition: an experiment under mobile bed conditions." *Sedimentology*, 52(3), 627-649.

Schwämmle, V., and Herrmann, H. J. (2003). "Solitary wave behaviour of sand dunes." *Nature*, 426(6967), 619-620.

Venditti, J. G., Church, M. A., and Bennett, S. J. (2005). "On the transition between 2D and 3D dunes." *Sedimentology*, 52(6), 1343-1359.

Yalin, M. S. (1992). *River Mechanics*, Pergamon Press. Inc. New York, New York, U.S.A.